magnetochemistry

MDPI

Article

Structural, Elastic, Electronic, and Magnetic Properties of Full-Heusler Alloys Sc_2TiAl and Sc_2TiSi Using the FP-LAPW Method

Khadejah M. Al-Masri [1], Mohammed S. Abu-Jafar [1,*], Mahmoud Farout [1,*], Diana Dahliah [1], Ahmad A. Mousa [2,3], Said M. Azar [4] and Rabah Khenata [5]

1 Department of Physics, An-Najah National University, Nablus P.O. Box 7, Palestine
2 Department of Basic Sciences, Middle East University, Amman 11831, Jordan
3 Applied Science Research Center, Applied Science Private University, Amman 11831, Jordan
4 Department of Physics, Faculty of Science, Zarqa University, Zarqa 13132, Jordan
5 Laboratoire de Physique Quantique et de Modélisation Mathématique de la Matière (LPQ3M), Université de Mascara, Mascara 29000, Algeria
* Correspondence: mabujafar@najah.edu (M.S.A.-J.); m.qaroot@najah.edu (M.F.)

Abstract: In this article, the structural, elastic, electronic, and magnetic characteristics of both regular and inverse Heusler alloys, Sc_2TiAl and Sc_2TiSi, were investigated using a full-potential, linearized augmented plane-wave (FP-LAPW) method, within the density functional theory. The optimized structural parameters were determined from the minimization of the total energy versus the volume of the unit cell. The band structure and DOS calculations were performed within the generalized gradient approximation (GGA) and modified Becke–Johnson approaches (mBJ-GGA), employed in the Wien2K code. The density of states (DOS) and band structure (BS) indicate the metallic nature of the regular structure of the two compounds. The total spin magnetic moments for the two compounds were consistent with the previous theoretical results. We calculated the elastic properties: bulk moduli, *B*, Poisson's ratio, ν, shear modulus, S, Young's modulus (Y), and the B/s ratio. Additionally, we used Blackman's diagram and Every's diagram to compare the elastic properties of the studied compounds, whereas Pugh's and Poisson's ratios were used in the analysis of the relationship between interatomic bonding type and physical properties. Mechanically, we found that the regular and inverse full-Heusler compounds Sc_2TiAl and Sc_2TiSi were stable. The results agree with previous studies, providing a road map for possible uses in electronic devices.

Keywords: Heusler alloy; band structure; elastic constant; magnetic order; FP-LAPW

Citation: Al-Masri, K.M.; Abu-Jafar, M.S.; Farout, M.; Dahliah, D.; Mousa, A.A.; Azar, S.M.; Khenata, R. Structural, Elastic, Electronic, and Magnetic Properties of Full-Heusler Alloys Sc_2TiAl and Sc_2TiSi Using the FP-LAPW Method. *Magnetochemistry* **2023**, *9*, 108. https://doi.org/10.3390/magnetochemistry9040108

Academic Editors: Devashibhai Adroja and Dmitry Alexandrovich Filippov

Received: 16 February 2023
Revised: 8 April 2023
Accepted: 13 April 2023
Published: 16 April 2023

1. Introduction

The discovery of Heusler compounds has been greatly applied in spintronics, shape memory, thermoelectrics, and a tremendous domain of functionalities. Changing elements afforded Heusler alloys multiple functionalities, which led to a broad range of interest [1–8].

Heusler alloys could be categorized into four groups: (i) Full Heusler alloys (FHAs), with the chemical formula X_2YZ, crystallize in the regular Heusler ($L2_1$)(225) crystal structure with the prototype $AlCu_2Mn$, when the valence number of Y is less than that of X. (ii) The inverse Heusler (Xa)(216), which has the same chemical formula as full Heusler, but it crystallizes in the $C1_b$ type with prototype $CuHg_2Ti$, where the valence number of Y is greater than that of X. (iii) Half-Heusler alloys (HHAs) have the chemical formula XYZ, crystalline in the $C1_b$ structure, as an inverse Heusler with one X missing. (iv) Quaternary Heusler alloys (QHAs) have the chemical formula XX′YZ, crystalline in the LiMgPdSn (Y-type). In all categories, X, X′, and Y are transition metals, while Z is the main-group element.

Heusler compounds and other half-metallic compounds have been the subject of several previous studies utilizing a variety of computational and experimental techniques.

In 2019, Han et al. [9] performed a study on 171 scandium-based full Heusler compounds. They found that the $L2_1$-type structure (regular structure) is more stable than the Xa structure (inverse structure) since the energy difference between the two structures ($E = E_{XA} - E_{L21}$) is greater than zero. This means that the $L2_1$-type structure is more likely to be synthesized. They also calculated the band structure of Sc_2TiAl and Sc_2TiSi alloys using the first-principle calculations. The calculated electronic structures of the $L2_1$-type structure and the Xa structure of Sc_2TiAl and Sc_2TiSi are ferromagnetic.

Full Heusler compounds are intermetallic compounds that have the composition X2YZ, where X and Y are transition metals and Z is a main-group element. These compounds have attracted significant attention due to their interesting electronic, magnetic, and thermoelectric properties. Among the various types of full Heusler compounds, metallic full Heusler compounds have attracted significant attention due to their high electrical conductivity, which makes them suitable for electronic applications [10–14].

Several studies have explored the properties and potential applications of metallic full Heusler compounds. Graf et al. [15] discussed the simple rules for understanding the crystal structure of Heusler compounds. Felser and Hirohata [16] highlighted the potential of Heusler compounds for spintronics and related applications. Nayak et al. [17] provided a comprehensive review of computational and experimental studies on half-metallic Heusler compounds, including Mn_2PtGa. These studies demonstrate the growing interest in metallic full Heusler compounds and the potential they hold for various applications [15–17].

A review on the recent development and future perspectives has been conducted by Elphick et al. [18]. Wu et al. investigated the mechanical properties of various Co_2-based Heusler compounds by calculating their elastic constants using a full-potential all-electron method [19].

Recently, Yahya et al. computationally investigated the structural, electronic, and elastic properties of Co_2CrAl and Cr_2MnSb Heusler alloys. The results revealed that both compounds have half-metallic characters [20]. In 2020, Abu Baker et al. [21] used the FP-LAPW approach to explore the structural, electronic, magnetic, and elastic properties of the regular Co_2TiSn and inverse Co_2TiSn full Heusler alloys. The inverse Zr_2RhGa and regular Co_2TiSn have lattice parameters of 6.619 Å and 6.094 Å, respectively. Additionally, it was discovered that these compounds have total magnetic moments of 1.9786 μ_B and 1.99 μ_B, respectively. Furthermore, the indirect energy gaps for these compounds are 0.482 eV and 0.573 eV, respectively. They are also mechanically stable. On the other hand, Alrahamneh et al. calculated the thermoelectric properties for Zr_2RhGa and Zr_2RhIn compounds, and they found that both compounds exhibit half-metallic behavior and are unsuitable for thermoelectric applications [5].

In 2021, Yotong Li et al. [22] screened the half-metallic X_2Y (Al/Si) full Heusler alloys based on first-principle calculations. There are 26 stable alloys, out of which 24 are magnetic and 10 are half-metallic. For alloys with magnetism, DOS were calculated by applying the GGA. The $(Ag/Cu/Mg)_2Y(Al/Si)$ alloys were found to be unstable, while (Mn/Co)2Y(Al/Si) alloys are always stable. $X_2Cr(Al/Si)$ alloys are stable, while $X_2Nb(Al/Si)$ alloys are always unstable. The $(Co/Mn)_2YZ$ alloys always exhibit magnetism and half-metallicity. Moreover, they predicted that $(Mn/Co)_2Y(Al/Si)$ alloys can be considered as candidates for spintronic devices and serve as a valuable reference for future experimental work.

The main purpose of this work is to investigate and predict the structural, magnetic, electronic, and elastic properties of Sc_2TiAl and Sc_2TiSi in the cubic phase for possible spintronic applications. Spintronics reveals a possible high capacity for next-generation information technology [23]. To determine if our compounds are suitable for spintronics, we have studied various properties using the FP-LAPW method.

The motivation of the present study is to examine the mechanical properties of the compounds and analyze their stability by investigating their behavior. Considering the limited availability of theoretical and experimental data on this topic, it is crucial to validate the findings reported in [9].

This work is divided into four sections. The first section has provided an introduction that highlighted the importance of Heusler alloys and a literature review about Sc_2TiAl and Sc_2TiSi specifically, and Heusler alloys generally, in addition to outlining the main purpose of this work. The second section describes the computational method used. The third section presents the results obtained by referring to other results available in the literature review; therefore, all the results obtained are systematically compared. The last section is a conclusion, that summarizes the physical properties of the regular and inverse Sc_2TiAl and Sc_2TiSi compounds.

2. Computational Method

In this work, the density functional theory (DFT) calculations were carried out using the full-potential, linearized augmented plane-wave (FP-LAPW) technique, as implemented in the WIEN2k package [24]. The generalized gradient approximation, parameterized by Perdew, Burke, and Ernzerhof (GGA-PBE) [25], was used to calculate the structural parameters, namely the lattice parameters and the bulk modulus. The GGA-PBE method depends on the local gradient of the electronic density, in addition to the value of the density, providing a more accurate description of variations in the electron–electron interactions. The GGA-PBE functional calculations mostly underestimate the energy bandgap values; therefore, a modified Becke–Johnson (mBJ-GGA) functional [26,27] might be used to enhance the energy bandgap values. For Sc_2TiAl, the muffin-tin (MT) radii of Sc, Ti, and Al atoms are 2.50, 2.50, and 2.39 a.u., respectively, whereas, for Sc2TiSi, Sc, Ti, and Si atoms are 2.45, 2.45, and 2.14 a.u., respectively. To obtain a self-consistency for Sc_2TiAl and Sc_2TiSi, 1240 special k-points in the irreducible Brillion zone (IBZ) were used with a grid equivalent to 50,000 k-points in the full BZ [28]. Furthermore, the expansions of the wave functions were set to $l = 10$ inside the MT spheres and the number of plane waves was restricted by $K_{max} \times R_{MT} = 8$. The self-consistent calculations were considered to converge only when the calculated total energy of the crystal converged to less than 0.01 mRy. Finally, using the second-order derivative within the IRelast formalism [29], the elastic constants were calculated.

3. Results

3.1. Structural Properties

To calculate the optimized structural properties: lattice constant (a), bulk modulus (B), its pressure derivative (B'), and minimum energy, E_0, the total energy (in Ry) versus volume (in a.u^3) graphs were fitted using Murnaghan's equation of state (EOS), which is given by [30,31]:

$$E(V) = E_0 + \frac{VB}{B'}\left\{\left[\frac{\left(\frac{V_0}{V}\right)^{B'}}{B'-1}\right]+1\right\} - \frac{BV_0}{B'-1} \quad (1)$$

where pressure, $P = -\frac{dE}{dV}$, and bulk modulus, $B' = -V\frac{dP}{dV} = V\frac{d^2E}{dV^2}$.

The regular Heusler Sc_2TiAl and Sc_2TiSi compounds have the space group Fm-3m $L2_1$ (225), while the inverse Heusler Sc_2TiAl and Sc_2TiSi compounds have the space group F-43m Xa (216) [1]. Figure 1 shows the crystal structures of the full Heusler Sc_2TiAl and Sc_2TiSi compounds.

In the optimized volume calculation, an estimated value of the lattice parameter was used for each compound, and the total energy versus the volume of Sc_2TiAl and Sc_2TiSi alloys is shown in Figures 2 and 3. Figure 2 indicates that the regular Sc_2TiAl has a minimum energy, E_0, lower than the inverse Sc_2TiAl, indicating that the regular structure of Sc_2TiAl is more mechanically stable than the inverse structure. Similarly, Figure 3 demonstrates that the regular Sc_2TiSi has a minimum energy, E_0, lower than the inverse Sc_2TiSi implying that the regular structure of Sc_2TiSi is more mechanically stable than the inverse structure.

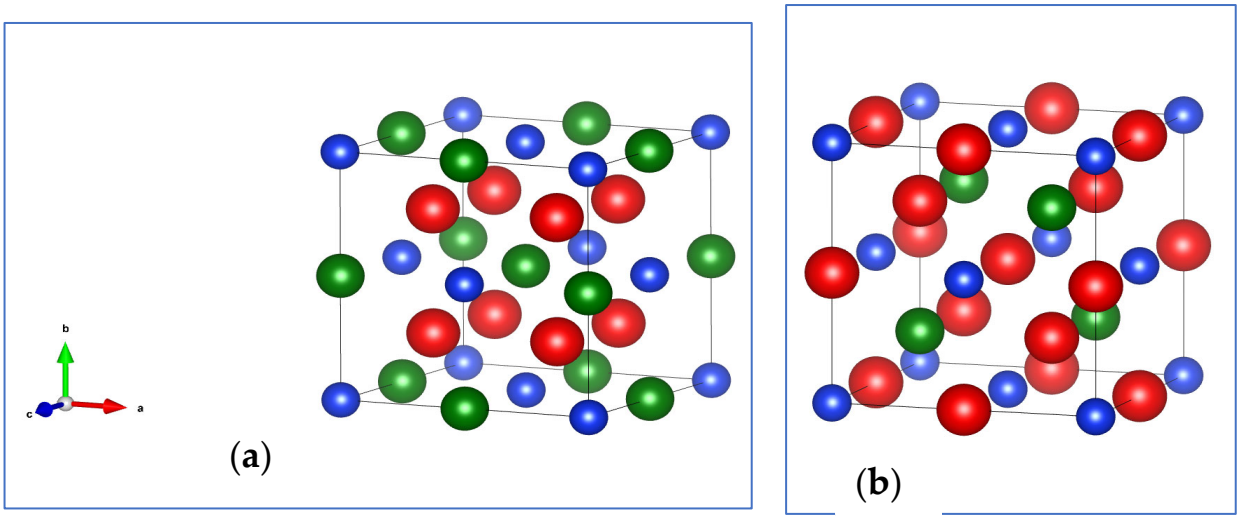

Figure 1. Crystal structures of Sc_2TiAl and Sc_2TiSi in (**a**) regular Heusler ($L2_1$) and (**b**) inverse Heusler (Xa) (Red: Sc, Green: Ti, Blue: Al/Si).

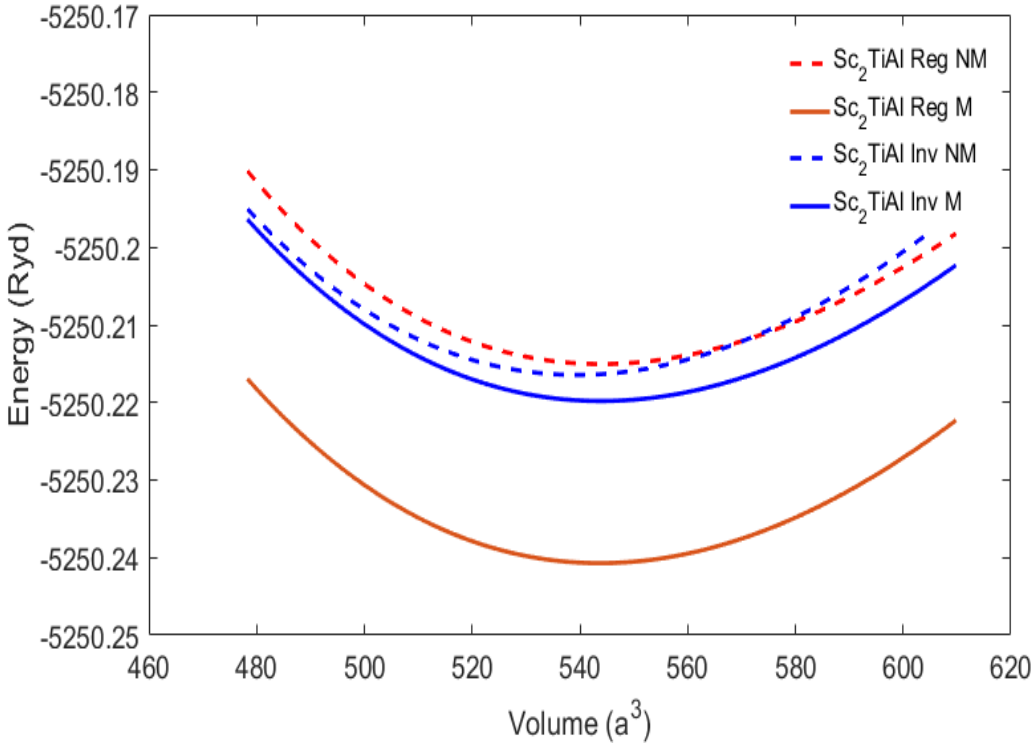

Figure 2. The total energy (Ry) versus volume ($a.u^3$) of non-magnetic, regular, and inverse Sc_2TiAl Heusler.

The calculated structural parameters of the regular and the inverse Sc_2TiAl and Sc_2TiSi are listed in Table 1. The table demonstrates that the present calculated lattice constants are compatible with the previous theoretical results for both the regular and inverse Heusler structures of Sc_2TiAl and Sc_2TiSi [9].

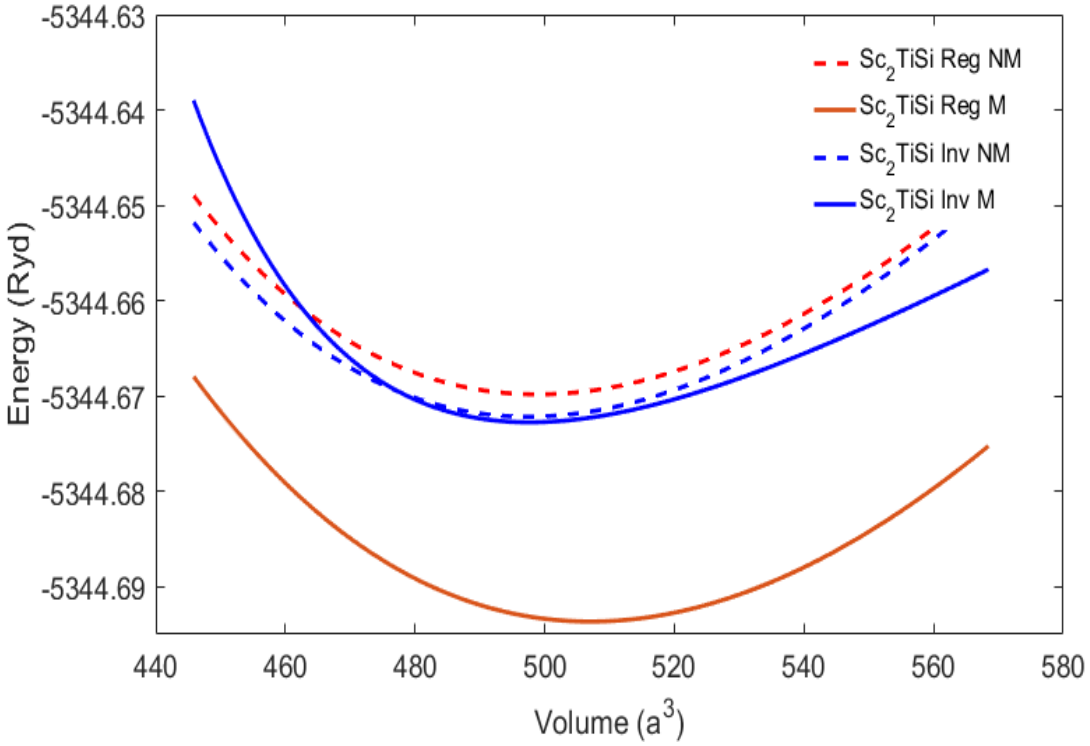

Figure 3. The total energy (Ry) versus volume (a.u^3) of non-magnetic, regular, and inverse Sc_2TiSi Heusler.

Table 1. The obtained lattice constant (a), bulk modulus (B), pressure derivative of the bulk modulus (B'), minimum energy (E_0), and formation energy (E_f) for the regular and inverse Heusler of both Sc_2TiAl and Sc_2TiSi.

Structure	Space Group	Reference	a (A^0)	B (GPa)	B' (GPa)	E_0 (eV)	E_f (meV)
Sc_2TiAl	Fm-3m (225)	Present	6.88	75.9	2.59	−5250.241	−391.1
		Theoretical	6.87 [9]				
	F-43m (216)	Present	6.84	73.9	3.30	−5250.219	−109.8
		Theoretical	6.83 [9]				
Sc_2TiSi	Fm-3m (225)	Present	6.69	85.28	4.35	−5344.693	−913.3
		Theoretical	6.69 [9]				
	F-43m (216)	Present	6.64	82.79	5.26	−5344.669	−584.7
		Theoretical	6.64 [9]				

3.2. Formation Energy

In this section, we show how to calculate the formation energy of the Sc_2TiX (X = Si and Al) compounds in both regular and inverse structures. The formation energy (E_f) is defined as the difference between the total energy of a compound and the energy of its components, and is given by the following formula [32]:

$$E_f = E_{Sc_2TiX} - \left(2E_{Sc}^{hex} + E_{Ti}^{hex} + E_X\right) \quad (2)$$

Here, E_{Sc_2TiX} represents the total energy of the Sc_2TiX compound in the structure being studied, while E_{Sc}^{hex} and E_{Ti}^{hex} represent the energy of scandium and titanium in hexagonal structures, respectively. Additionally, E_X represents the energy for aluminum (face-centered cubic) and silicon (diamond structure). The calculated values of E_f are listed in Table 1.

The formation energy indicates the stability of the compound and the extent of its natural formation [5]. A negative value means that the compound could be naturally formed. Based on Table 1, we observe that the formation energy of Sc_2TiAl and Sc_2TiSi compounds are negative in both regular and inverse structures, with the regular structure being the most stable for both systems. This is because the formation energy is less than that of the inverse structure. As the formation energy decreases, the stability of the compound increases. Therefore, we can conclude that the Sc_2TiX compounds exist in nature in the regular structure.

3.3. Magnetic Properties

The total and atom-resolved spin magnetic moments for the regular and inverse Heusler compounds Sc_2TiAl and Sc_2TiSi were calculated, and the results were compared with those of other theoretical works, as shown in Table 2. As indicated in Table 2, we concluded that the computed total spin magnetic moment (MM^{tot}) of the regular and inverse Heusler compounds Sc_2TiAl and Sc_2TiSi is reasonably comparable to the findings of prior theoretical studies [9].

Table 2. Total, atom-resolved, and interstitial spin magnetic moments for inverse and regular Sc_2TiAl and Sc_2TiSi.

Structure	Reference	Magnetic Moment in μ_B					
		Sc	**Sc**	**Ti**	**Al**	**Interstitial**	**MM^{tot}**
Regular Sc_2TiAl	Present Theoretical	0.38	0.38	1.71	−0.04	0.43	2.86 2.92 [9]
Inverse Sc_2TiAl	Present Theoretical	0.18	0.42	0.91	−0.02	0.60	2.09 2.24 [9]
Regular Sc_2TiSi	Present Theoretical	0.33	0.33	1.60	−0.05	0.76	2.97 2.96 [9]
Inverse Sc_2TiSi	Present Theoretical	0.20	0.63	1.05	−0.04	0.70	2.54 2.51 [9]

The MM^{tot} for the regular Sc_2TiAl was 2.72 μ_B, while it was 2.07 μ_B for the inverse Sc_2TiAl. The MM^{tot} in the inverse structure is lower than that in the normal structure due to the low contribution of the Ti atom in the inverse case, whereas its contribution was higher in the normal case. Therefore, it can be noted from the results produced here that the regular and inverse Sc_2TiAl compound's computed MM^{tot} values are close to the prior theoretical findings [9].

Table 2 shows the results for the regular and inverse Heusler Sc_2TiSi compounds. The main contribution in the MM^{tot} was due to the high contribution of the Ti atom in the regular case, while its contribution was lower by ∼34% in the inverse case, which caused the MM^{tot} to be lower (MM^{tot} = 2.204 μ_B) in the inverse case compared to the case of regular Heusler Sc_2TiSi (MM^{tot} = 2.808 μ_B). It was noticed that the atoms that occupied the Z position in X_2YZ or XYXZ structures for both molecules Sc_2TiAl and Sc_2TiSi did not significantly contribute to the MM^{tot}. The non-integral total magnetic moment of both compounds confirmed their metallic nature and was consistent with the results of their band structures and DOS. Based on the magnetic results, our studied compounds are unlikely to be half-metallic.

3.4. Electronic Structure

In this section, we investigated both the partial and total density of states (PDOS, TDOS) and the band structure (BS) for both Sc_2TiAl and Sc_2TiSi alloys. Since the regular $L2_1$ cubic structure is the ground state, we will focus on the regular $L2_1$ electronic structure. The analysis of the BS for regular Heusler structures of Sc_2TiAl and Sc_2TiSi showed that

they exhibited metallic behavior for both spin-up and spin-down within the GGA-PBE and mBJ-GGA methods, with zero-energy gaps, as shown in Figure 4.

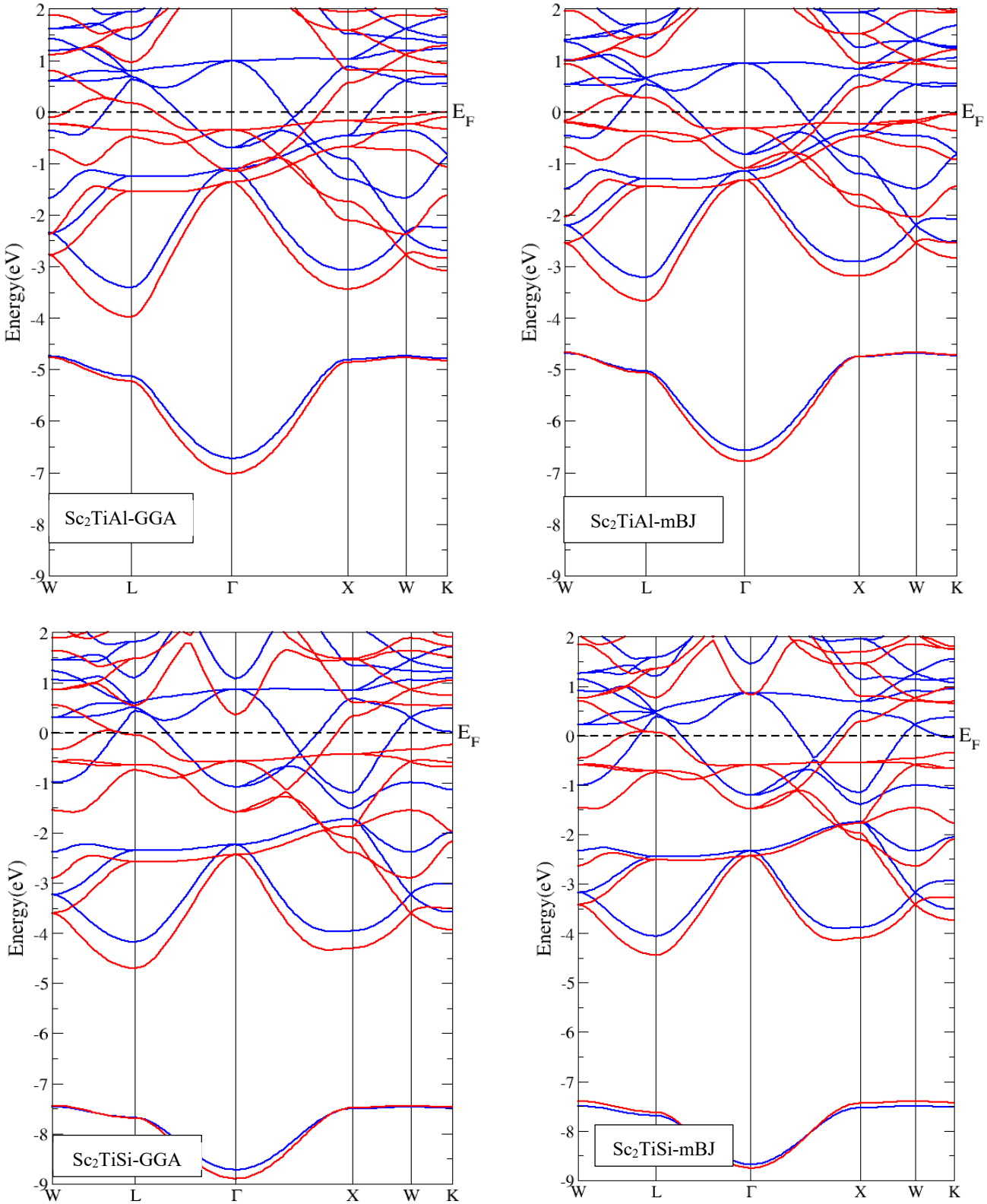

Figure 4. Calculated band structure for regular Sc_2TiAl and Sc_2TiSi using GGA and mBJ (blue lines for spin-up, red lines for spin-down).

Figures 5 and 6 show the TDOS and PDOS for the spin-up and spin-down of regular Sc_2TiAl and Sc_2TiSi Heusler alloys. These figures also show the metallic behavior for both alloys.

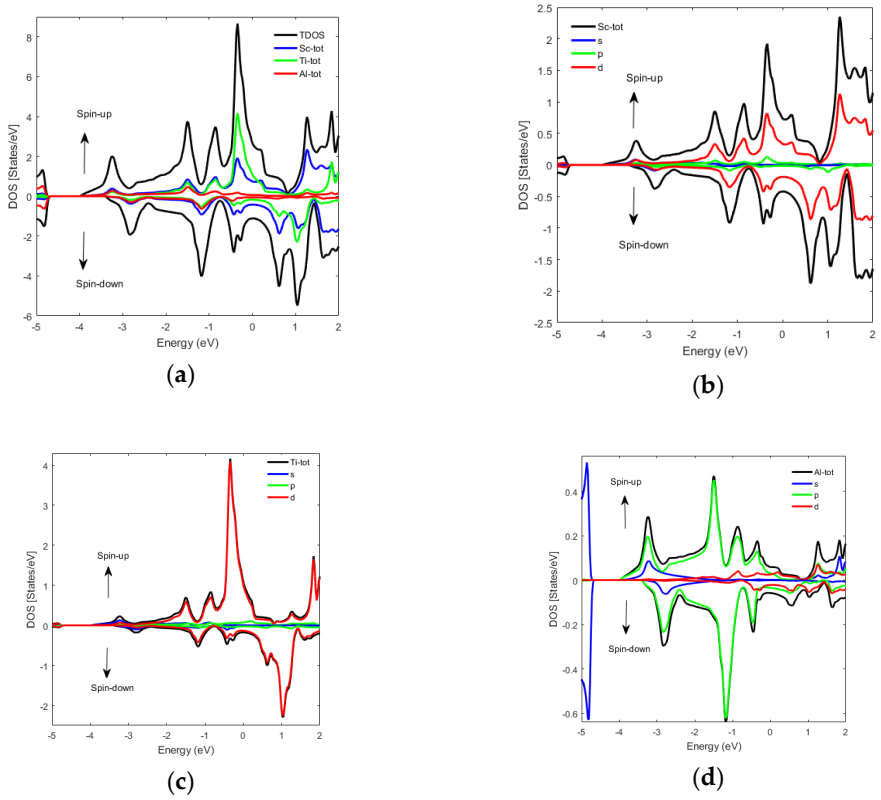

Figure 5. (**a**) TDOS for regular Sc_2TiAl, and PDOS for the (**b**) Sc atom, (**c**) Ti atom, and the (**d**) Al atom.

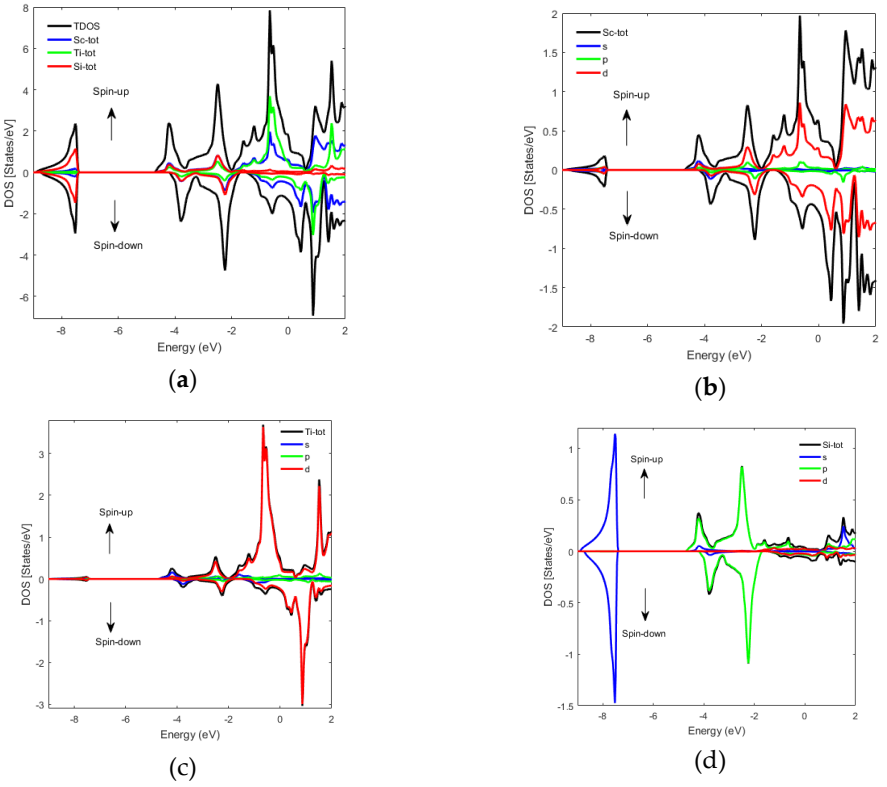

Figure 6. (**a**) TDOS for regular Sc_2TiSi, and PDOS for the (**b**) Sc atom, (**c**) Ti atom, and the (**d**) Si atom.

In the spin-up regular Sc_2TiAl (Figure 5), the main contributions to the valence band (VB) and conduction band come from the Sc-d state, the Ti-d state, and both the s- and p-states of Al. The main contributions come from the Ti atom, then the Sc atom, and then a small contribution from the Al atom in this compound. In addition, the main contributions to the conduction band come from the Sc-d state, the Ti-d state, and the s- and p-states of Al, with the main contributions coming from the Sc atom, then the Ti atom, and then a small contribution from the Al atom in this compound. In spin-down of regular Sc_2TiAl (Figure 5), the main contributions to the valence band come from the Sc-d state, the Ti-d state, and the s- and p-states of Al, with the main contributions coming from the Sc atom, then a small contribution from the Al atom, and then the Ti atom in this compound. The main contributions to the conduction band come from the Sc-d state, the Ti-d state, and the s- and p-states of Al, with the main contributions coming from the Sc atom, then the Ti atom, and then a small contribution from the Al atom in this compound.

In the spin-up and spin-down states of regular Sc_2TiSi (Figure 6), the Sc-d and Ti-d states, as well as the s- and p-states of Si, make the main contributions to the valence and conduction bands.

3.5. Elastic Properties

In this study, we investigated the bulk modulus (B), shear modulus (S), elastic constants (C_{ij}), Bugh ratio (B/S), Poisson's ratio (ν), Young's modulus (Y), and the anisotropic factor (A) for the regular and inverse Heusler alloys Sc_2TiAl and Sc_2TiSi. To investigate the stability, we computed three symmetry elements, C_{11}, C_{12}, and C_{44}, for cubic bulk alloys. The Born–Huang criteria of mechanical stability are as follows [33–35]:

$$\begin{gathered} C_{11} > 0, \\ C_{44} > 0, \\ C_{11} + 2C_{12} > 0, \\ C_{11} - C_{12} > 0, \\ C_{11} > B > C_{12} \end{gathered} \tag{3}$$

where the bulk C_{44}-shear, and the tetragonal shear moduli, C', must be positive [19]. The third criterion is known as the spinodal pressure, $p_s = C_{11} + 2C_{12}$, while the last criterion is used to define an additional elastic constant, called the tetragonal shear modulus:

$$C' = C_{11} - C_{12} \tag{4}$$

Tetragonal stability is achieved when the hydrostatic pressure becomes $2p > C'$.

The Cauchy pressure for cubic crystals is given by the relation [19]:

$$Pc = C_{12} - C_{44} \tag{5}$$

Based on the investigated compounds and the mechanical stability conditions mentioned above, both the regular and inverse structures of Sc_2TiAl and Sc_2TiSi were stable (see Table 3).

Table 3. Elastic constants (C_{ii}), bulk modulus (B), and anisotropic factor (A) of Sc_2TiAl and Sc_2TiSi.

Compound	C_{11} (GPa)	C_{12} (GPa)	C_{44} (GPa)	B (GPa)	A
Regular Sc_2TiAl	96.914	67.463	63.778	77.280	4.331
Inverse Sc_2TiAl	75.932	73.512	63.281	74.318	52.298
Regular Sc_2TiSi	106.781	81.347	64.582	89.825	5.078
Inverse Sc_2TiSi	95.248	94.762	63.792	94.924	262.519

Afterwards, the ductile behavior and the type of chemical bonds were investigated. We found that compounds with a Pugh ratio of $B/S > 1.75$ and $\nu > 0.26$ were ductile, while others were brittle [36–39]. The Voigt shear modulus, S_v, the Reuss shear modulus, S_R, the Hill shear modulus, S_H, and the bulk modulus, B, were calculated using the following equations [40–42]:

$$S_v = \frac{1}{5}(C_{11} - C_{12} + 3C_{44}), \tag{6}$$

$$S_R = 5C_{44}(C_{11} - C_{12})(4C_{44} + 3(C_{11} - C_{12})), \tag{7}$$

$$S_H = 0.5(S_v + S_R) \tag{8}$$

$$B = \frac{1}{3}(C_{11} + 2C_{12}), \tag{9}$$

The nature of bonding is indicated by the ν value. Compounds with covalent bonds have a ν value smaller than 0.25, while for compounds with ionic bonds, the ν value is between 0.25 and 0.5 [34–36]. According to Table 4, the regular and inverse Heusler compounds Sc_2TiAl and Sc_2TiSi are ductile, and they have dominant ionic bonds.

$$\nu = \frac{3B - 2S}{2(3B + S)}, \tag{10}$$

or

$$\nu = \frac{c_{12}}{c_{11} + c_{12}} \tag{11}$$

Table 4. Shear modulus (S), B/S ratio, Voigt Poisson's ratio (ν), and Young's modulus (Y) of Sc_2TiAl and Sc_2TiSi.

Compound	*S* (GPa)	*B*/*S* (GPa)	*Y* (GPa)	ν
Regular Sc_2TiAl	45.41	1.70	113.30	0.247
Inverse Sc_2TiAl	38.45	1.93	98.39	0.279
Regular Sc_2TiSi	43.84	2.05	113.11	0.290
Inverse Sc_2TiSi	38.37	2.74	101.45	0.321

The third and fourth criterions in Equation (1) restrict the range of Poisson's ratio to $-1 \leq \nu \leq 1/2$.

Young modulus (Y) (the ratio between stress and strain) is given by the following:

$$Y = \frac{9BS}{(S + 3B)}. \tag{12}$$

The anisotropic factor is given by:

$$A = \frac{2C_{44}}{C_{11} - C_{12}}. \tag{13}$$

The cubic elastic anisotropy or the Zener ratio can be used as physical quantities to describe the structural stability of a material. Materials with large Zener ratios tend to deviate from cubic structures. Materials with negative Zener ratios are mechanically unstable since they violate at least one of the stability criteria [19].

The hardness of materials is measured by the B and S moduli [43], while the stiffness of materials is measured by Young's modulus (Y). In addition, the elastic anisotropy, A, is a parameter used to measure the degree of anisotropy of the materials [44]. The elastic anisotropy (A) equals one for an isotropic alloy, while any value other than one indicates elastic anisotropy [45]. The inverse and regular Heusler Sc_2TiAl and Sc_2TiSi compounds exhibit elastic anisotropy, as shown in Table 3.

Table 3 shows that both Sc_2TiAl and Sc_2TiSi, in both regular and inverse structures, satisfy the stability conditions and are considered mechanically stable with elastic anisotropy. Table 4 shows that the regular and inverse structures of Sc_2TiSi are ductile, as $B/S > 1.75$ and $\nu > 0.26$. However, the regular structure of Sc_2TiAl is brittle ($B/S < 1.75$ and $v < 0.26$), while the inverse structure is ductile ($B/S > 1.75$ and $\nu > 0.26$).

Blackman's and Every's diagrams are used due to their efficiency in comparing the elastic properties of cubic materials. These diagrams correlate dimensionless quantities that are related to ratios of different moduli. Figure 7 summarizes the results of this study in such diagrams. Blackman's diagram compares $F_{12} = \frac{c_{12}}{c_{11}}$ to $F_{44} = \frac{c_{44}}{c_{11}}$, while Every's diagram is more complicated. It compares $s_3 = (c_{11} - c_{12} - 2\,c_{44})/\,(c_{11} + 2\,c_{44})$ as a function of $s_2 = (c_{11} - c_{44})/\,(c_{11} + 2\,c_{44})$. Materials with $s_3 = 0$ are isotropic, and the two quantities, s_2 and s_3, are related to the elastic waves. Since $c_{44} > 0$, then $F_{44} > 0$, whereas F_{12} is restricted to $-0.5 < F_{12} < 1$. These are the restrictions for Blackman's diagram, and all values within these ranges are allowed. In Every's diagram, the values for stability are restricted to fall into the triangle with (s_2, s_3), equal to (-0.5, -1)–(1, 0)–(1, 1.5), as shown in Figure 7. It is noticed that the studied compounds in this study were below the isotropy line, where $s_3 = 0$ [19].

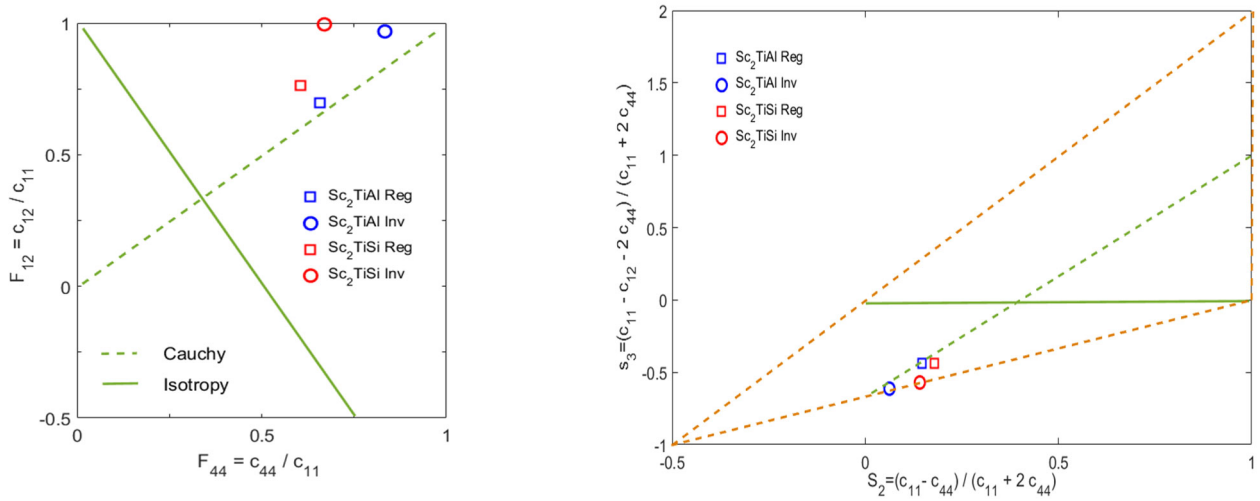

(**a**) (**b**)

Figure 7. (**a**) Blackman's and (**b**) Every's diagrams. The full green line refers to the isotropic case, where $A_e = 1$, and the dashed green line refers to the case where Cauchy pressure = 0. In Every's diagram, the stability triangle is marked by dashed brown lines.

From both diagrams, it can be noticed that the studied compounds were close to the Cauchy line, where $p_s = 0$. Additionally, all the studied compounds were in the region where the anisotropy index is positive [19].

Pettiford proposed a criterion that suggests that when Cauchy pressure is positive, it indicates that the compound has metallic bonding, whereas negative Cauchy pressure indicates covalent bonding in the compound. According to Pugh's criterion, materials are brittle when $k \leq 1.75$, where $k = B/S$, and materials are ductile when $k \geq 1.75$. Figure 8 shows a plot of the Cauchy pressure as a function of Pugh's ratio, with the two criteria depicted as horizontal and vertical lines.

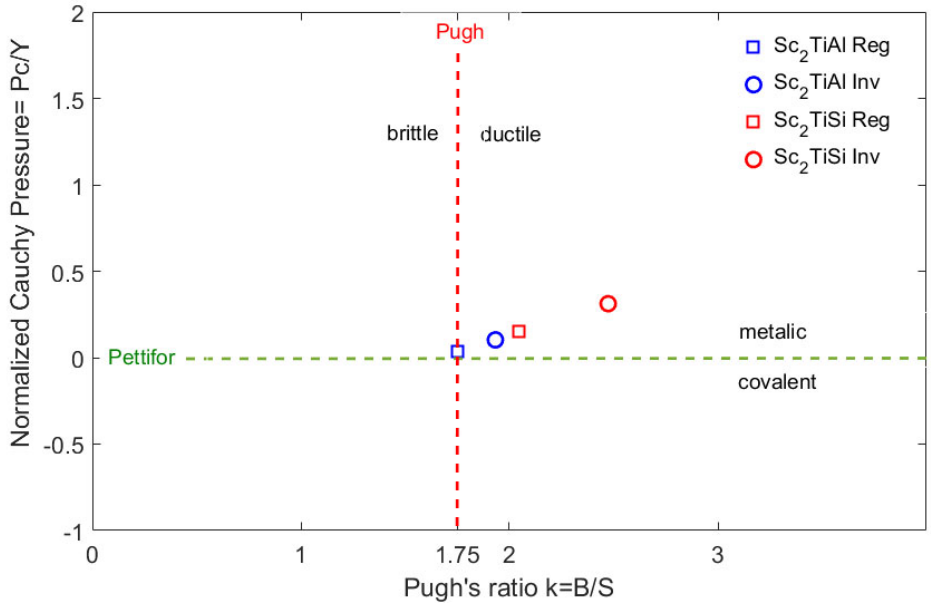

Figure 8. Ductile–brittle diagram for the studied compounds. The horizontal dashed line corresponds to the metallic-covalent criteria of Pettiford, and the vertical dashed line corresponds to the brittleness–ductile criteria of Pugh.

All studied compounds were classified as ductile and metallic materials, except the regular compound of Sc_2TiAl (k = 1.7), which lay slightly to the left of the vertical line between brittle and ductile. Therefore, it was considered a brittle compound.

4. Conclusions

This article scrutinized the structural, magnetic, electronic, and elastic properties of both Sc_2TiAl and Sc_2TiSi. The results were as follows: According to the electronic properties, both regular Heusler Sc_2TiAl and Sc_2TiSi compounds are metals with zero-energy bandgaps in both GGA-PBE and mBJ methods. As for the magnetic properties, both Sc_2TiAl and Sc_2TiSi alloys are ferromagnetic compounds with a total magnetic moment of MM^{tot} =2.86, 2.09, 2.97, and 2.54 μ_B, respectively. Additionally, the elastic properties of these compounds emphasized that both regular and inverse Sc_2TiAl and regular Sc_2TiSi are mechanically stable. The B/S ratios showed that both regular and inverse Heusler Sc_2TiAl and Sc_2TiSi compounds have ductile natures. Moreover, the Poisson's ratio values indicated that both Sc_2TiAl and Sc_2TiSi alloys have ionic bonds. Finally, both Sc_2TiAl and Sc_2TiSi compounds exhibited elastic anisotropy.

Author Contributions: Conceptualization, M.S.A.-J.; project administration, M.S.A.-J.; supervision, M.S.A.-J. and M.F.; investigation, K.M.A.-M., M.S.A.-J., D.D., A.A.M. and R.K.; data curation, K.M.A.-M., M.F., D.D. and A.A.M.; formal analysis, K.M.A.-M., M.F., A.A.M. and R.K.; methodology, K.M.A.-M., M.F., M.S.A.-J., D.D., A.A.M. and S.M.A.; software, K.M.A.-M., M.F., D.D., S.M.A. and A.A.M.; writing—original draft, K.M.A.-M. and M.F.; visualization, M.S.A.-J. and R.K.; writing—review and editing, M.S.A.-J., A.A.M., S.M.A. and R.K.; validation, M.S.A.-J., A.A.M., S.M.A. and R.K. All authors have read and agreed to the published version of the manuscript.

Funding: This research received no external funding.

Institutional Review Board Statement: Not applicable.

Informed Consent Statement: Not applicable.

Data Availability Statement: The data that support the findings of this study are available from the corresponding author upon reasonable request.

Conflicts of Interest: The authors declare that they have no known competing financial interest or personal relationships that could have appeared to influence the work reported in this paper.

References

1. Paudel, R.; Zhu, J. Investigation of half-metallicity and magnetism of (Ni/Pd/Ru) ZrTiAl quaternary Heusler alloys for spintronic applications. *Phys. Condens. Matter* **2019**, *557*, 45–51. [CrossRef]
2. Azar, S.; Mousa, A.; Khalifeh, J. Structural, electronic and magnetic properties of Ti1+xFeSb Heusler alloys. *Intermetallics* **2017**, *85*, 197–205. [CrossRef]
3. Berrahal, M.; Bentouuaf, A.; Rached, H.; Mebsout, R.; Aissa, B. Investigation of Ruthenium based Full-Heusler compound for thermic, spintronic and thermoelectric applications: DFT computation. *Mater. Sci. Semicond. Process.* **2021**, *134*, 106047. [CrossRef]
4. Patel, P.; Pandaya, J.; Shinde, S.; Gupta, S.; Narayan, S. Investigation of Full-Heusler compound Mn2MgGe for magnetism, spintronics and thermoelectric applications: DFT study. *Comput. Condens. Matter* **2020**, *23*, e00472. [CrossRef]
5. Alrahamneh, M.; Mousa, A.; Khalifeh, J. First principles study of the structural, electronic, magnetic and thermoelectric properties of Zr_2RhAl. *Phys. Condens. Matter* **2019**, *552*, 227–235. [CrossRef]
6. Remil, G.; Zitouni, A.; Bouadjemi, B.; Houari, M.; Abbad, A.; Benstaali, W.; Cherid, S.; Matougui, M.; Lantri, T.; Bentata, S. A potential full Heusler thermoelectric material CO_2ZrZ (Z=Al, Si, Ga and Sn) in low temperature: An Ab-initio investigation. *Solid State Commun.* **2021**, *336*, 114422. [CrossRef]
7. Srivastava, V.; Kaur, N.; Khenata, R.; Dar, S. Investigation of the electronic, magnetic, elastic, thermodynamic and thermoelectric properties of Mn_2CoCr Heusler compound A DFT-based simulation. *J. Magn. Magn. Mater.* **2020**, *513*, 167107. [CrossRef]
8. Mushtaq, M.; Khalid, S.; Atif Sattar, M.; Khenata, R.; Seddik, T.; Ahmad Dar, S.; Muhammad, I.; Bin Omran, S. Electronic band structure, phase stability, magnetic and thermoelectric characteristics of the quaternary Heusler alloys CoCuZrAs and CoRhMoAl: Insights from DFT computations. *Inorg. Chem. Commun.* **2021**, *124*, 108384. [CrossRef]
9. Han, Y.; Chen, Z.; Kuang, M.; Liu, Z.; Wang, X.; Wang, X. 171 Scandium-based full Heusler compounds: A comprehensive study of competition between XA and L21 atomic ordering. *Results Phys.* **2019**, *12*, 435–446. [CrossRef]
10. Wang, C.; Casper, F.; Gasi, T.; Ksenofontov, V.; Balke, B.; Fecher, G.H.; Felser, C.; Hwu, Y.; Lee, J. Structural and magnetic properties of Fe2CoGa Heusler nanoparticles. *J. Phys. Appl. Phys.* **2012**, *45*, 295001. [CrossRef]
11. Shan, R.; Ouardi, S.; Fecher, G.H.; Gao, L.; Kellock, A.; Gloskovskii, A.; ViolBarbosa, C.E.; Ikenaga, E.; Felser, C.; Parkin, S.S.P. A p-type Heusler compound: Growth, structure, and properties of epitaxial thin NiYBi films on MgO(100). *Appl. Phys. Lett.* **2012**, *101*, 212102. [CrossRef]
12. Galanakis, I.; Şaşıoğlu, E. High T_C half-metallic fully-compensated ferrimagnetic Heusler compounds. *Appl. Phys. Lett.* **2011**, *99*, 052509. [CrossRef]
13. Nayak, A.K.; Shekhar, C.; Winterlik, J.; Gupta, A.; Felser, C. Mn2PtIn: A tetragonal Heusler compound with exchange bias behavior. *Appl. Phys. Lett.* **2012**, *100*, 152404. [CrossRef]
14. Wei, X.P.; Hu, X.R.; Liu, B.; Lei, Y.; Deng, H.; Yang, M.K.; Deng, J.B. Electronic structure and magnetism in full-Heusler compound Mn2ZnGe. *J. Magn. Magn. Mater.* **2011**, *323*, 1606. [CrossRef]
15. Graf, T.; Felser, C.; Parkin, S.S. Simple rules for the understanding of Heusler compounds. *Prog. Solid State Chem.* **2011**, *39*, 1–50. [CrossRef]
16. Felser, C.; Hirohata, A. Heusler Alloys Properties, Growth, Applications. In *Springer Series in Materials Science*; Springer: Berlin/Heidelberg, Germany, 2016; ISBN 978-3-319-21449-8.
17. Nayak, A.K.; Nicklas, M.; Chadov, S.; Shekhar, C.; Skourski, Y.; Winterlik, J.; Felser, C. Large zero-field cooled exchange-bias in bulk Mn2PtGa. *Phys. Rev. Lett.* **2013**, *110*, 127204. [CrossRef]
18. Elphick, K.; Frost, W.; Samiepour, M.; Kubota, T.; Takanashi, K.; Sukegawa, H.; Mitani, S.; Hirohata, A. Heusler alloys for spintronic devices: Review on recent development and future perspectives. *Sci. Technol. Adv. Mater.* **2021**, *22*, 235. [CrossRef]
19. Wu, S.-C.; Fecher, G.H.; Naghavi, S.S.; Felser, C. Elastic properties and stability of Heusler compounds: Cubic Co_2YZ compounds with L21 structure. *J. Appl. Phys.* **2019**, *125*, 082523. [CrossRef]
20. Yahya, S.J.; Abu-Jafar, M.S.; Al Azar, S.; Mousa, A.A.; Khenata, R.; Abu-Baker, D.; Farout, M. The Structural, Electronic, Magnetic and Elastic Properties of Full-Heusler Co_2CrAl and Cr_2MnSb: An Ab Initio Study. *Crystals* **2022**, *12*, 1580. [CrossRef]
21. Abu Baker, D.N.; Abu-Jafar, M.S.; Mousa, A.; Jaradat, R.; Ilaiwi, K.; Khenata, R. Structural, magnetic, electronic and elastic properties of half-metallic ferromagnetism full-Heusler alloys: Regular- Co_2TiSn and inverse- Zr_2RhGa using FP-LAPW method. *Mater. Chem. Phys.* **2020**, *240*, 122122. [CrossRef]
22. Li, Y.; Zhu, J.; Paudel, R.; Huang, J.; Zhou, F. Screen the half metallic X_2Y (Al/Si) full Heusler alloys based on the first principle calculations. *Comput. Mater. Sci.* **2021**, *193*, 110391. [CrossRef]
23. Oudrane, D.; Bourachid, I.; Bouafia, H.; Abidri, B.; Rached, D. Computational insights in predicting structural, mechanical, electronic, magnetic and optical properties of EuAlO3 cubic Perovskite using FP-LAPW. *Comput. Condens. Matter* **2021**, *26*, e00537. [CrossRef]
24. Blaha, P.; Schwarz, K.; Tran, F.; Laskowski, R.; Madsen, G.K.H.; Marks, L.D. WIEN2k: An APW+lo program for calculating the properties of solids. *J. Chem. Phys.* **2020**, *152*, 074101. [CrossRef]
25. Perdew, J.; Burke, K.; Ernzerhof, M. Generalized gradient approximation made simple. *Phys. Rev. Lett.* **1996**, *77*, 3865–3868. [CrossRef]

26. Becke, A.; Johnson, E. A simple effective potential for exchange. *J. Chem. Phys.* **2006**, *124*, 221101. [CrossRef] [PubMed]
27. Tran, F.; Blaha, P. Accurate band gaps of semiconductors and insulators with a semilocal exchange-correlation potential. *Phys. Rev. Lett.* **2009**, *102*, 226401. [CrossRef] [PubMed]
28. Blaha, P.; Schwarz, K.; Medsen, G.K.H.; Kvasnicka, D.; Luitz, J. *WIEN2k, An Augmented Plane Wave Plus Local Orbitals Program for Calculating Crystal Properties*; Vienna University Technology: Vienna, Austria, 2001. Available online: https://www.scirp.org/(S(i43dyn45teexjx455qlt3d2q))/reference/ReferencesPapers.aspx?ReferenceID=1880359 (accessed on 5 January 2023).
29. IRelast Package is Provided by M. Jamal as Part of the Commercial Code WIEN2K. 2014. Available online: http://www.wien2k.at/ (accessed on 5 January 2023).
30. Murnaghan, F.D. The compressibility of media under extreme pressures. *Proc. Natl. Acad. Sci. U.S.A.* **1944**, *30*, 244. [CrossRef]
31. Tyuterev, V.G.; Vast, N. Murnaghan's equation of state for the electronic ground state energy. *Comput. Mater. Sci.* **2006**, *38*, 350. [CrossRef]
32. Mousa, A.; Hamad, B.; Khalifeh, J. Structure, electronic and elastic properties of the NbRu shape memory alloys. *Eur. Phys. J.* **2009**, *72*, 575–581. [CrossRef]
33. Born, M.; Huang, K. Dynamical Theory of Crystal Lattices. *Am. J. Phys.* **1956**, *23*, 474. [CrossRef]
34. Gupta, Y.; Sinha, M.; Verma, S. Exploring the structural, elastic, lattice dynamical stability and thermoelectric properties of semiconducting novel quaternary Heusler alloy LiScPdPb. *J. Solid State Chem.* **2021**, *304*, 122601. [CrossRef]
35. Abu-Jafar, M.; Dayton-Oxland, R.; Jaradat, R.; Mousa, A.; Khenata, R. Structural, electronic, mechanical and elastic properties of Scandium Chalcogenides by first-principles calculations. *Phase* **2020**, *93*, 773. [CrossRef]
36. Pugh, S.F. Relations between the elastic moduli and the plastic properties of polycrystalline pure metals. *Philos. Mag.* **1954**, *45*, 823. [CrossRef]
37. Abu-Jafar, M.; Leonhardi, v.; Jaradat, R.; Mousa, A.; Al-Qaisi, S.; Mahmoud, N.; Bassalat, A.; Khenata, R.; Bouhemadou, A. Structural, electronic, mechanical, and dynamical properties of scandium carbide. *Results Phys.* **2021**, *21*, 103804. [CrossRef]
38. Cheriet, A.; Khenchoul, S.; Aissani, L.; Lagoun, B.; Zaabat, M.; Alhussein, A. First-principles calculations to investigate structural, magnetic, electronic and elastic properties of full-Heusler alloys Co2MB (M=V, Mn). *Solid State Commun.* **2021**, *337*, 114426. [CrossRef]
39. Abada, A.; Marbouh, N.; Bentayeb, A. First-principles calculations to investigate structural, elastic, electronic and magnetic properties of novel d half metallic half Heusler alloys XSrB (X=Be, Mg). *Intermetallics* **2022**, *140*, 107392. [CrossRef]
40. Voigt, W. *Ueber die Beziehung Zwischen den Beiden Elasticitätsconstanten Isotroper Körper*; Wiley Online Library: San Marcos, CA, USA, 1889; p. 38. [CrossRef]
41. Reuss, A. Berechnung der Fließgrenze von Mischkristallen auf Grund der Plastizitätsbedingung für Einkristalle. *Math Phys.* **1929**, *9*, 49. [CrossRef]
42. Hill, R. The Elastic Behaviour of a Crystalline Aggregate. *Proc. Phys. Soc.* **1952**, *65*, 349. [CrossRef]
43. Teter, D.M. Computational alchemy: The search for new superhard materials. *MRS Bull.* **1998**, *23*, 22. [CrossRef]
44. Zener, C. *Elasticity and Anelasticity of Metals*; University of Chicago Press: Chicago, IL, USA, 1948. [CrossRef]
45. Ravindran, P.; Fast, L.; Korzhavyi, P.A.; Johansson, B. Density functional theory for calculation of elastic properties of orthorhombic crystals: Application to $TiSi_2$. *J. Appl. Phys.* **1998**, *84*, 4891. [CrossRef]